View metadata, citation and similar papers at core.ac.uk

brought to you by CORE

provided by Edinburgh Research Explorer

THE UNIVERSITY of EDINBURGH

Edinburgh Research Explorer

Modular and Stackable Power Generators for Efficient Renewable Power Generation

Citation for published version:
Kails, K, Li, Q & Mueller, M 2019, 'Modular and Stackable Power Generators for Efficient Renewable Power Generation', *IET Renewable Power Generation*. https://doi.org/10.1049/iet-rpg.2019.0570

Digital Object Identifier (DOI):
10.1049/iet-rpg.2019.0570

Link:
Link to publication record in Edinburgh Research Explorer

Document Version:
Peer reviewed version

Published In:
IET Renewable Power Generation

General rights
Copyright for the publications made accessible via the Edinburgh Research Explorer is retained by the author(s) and / or other copyright owners and it is a condition of accessing these publications that users recognise and abide by the legal requirements associated with these rights.

Take down policy
The University of Edinburgh has made every reasonable effort to ensure that Edinburgh Research Explorer content complies with UK legislation. If you believe that the public display of this file breaches copyright please contact openaccess@ed.ac.uk providing details, and we will remove access to the work immediately and investigate your claim.

OPEN ACCESS

Download date: 23. Jul. 2021

Modular and Stackable Power Generators for Efficient Renewable Power Generation

Kevin Kails, Quan Li *, Markus Mueller

School of Engineering, Institute for Energy Systems, University of Edinburgh, EH9 3JL, UK
*Corresponding author: Quan Li, Quan.Li@ed.ac.uk

Abstract: Stackable power generators enable very compact electric machines with high power density. How to identify an effective way of stacking is necessary and requires new knowledge for future guidance. In this paper, both possibilities of stacking modules concentrically and axially are explored and compared. An axial flux generator based on our existing double claw pole design is used as a case study. The claw pole generator, which is modular and stackable, significantly benefits on-site installation due to its flexible small modules that can be easily transported. This is particularly important to the installation of offshore wind turbines. Superconducting field windings are applied instead of copper in such power generators, which greatly increases their power density. In order to further increase their power density and reduce mass, we improved the modularity of 5 MW generators and stacked them in both ways. Results show that the power density versus mass as well as volume can be improved through stacking the modules both concentrically and axially, while the former approach is much more effective. Stacking two modules of 5 MW concentrically results in a 12.1 MW power generator with a more compact structure and higher power density than the original 10 MW generator.

1. Introduction

One of the biggest challenges the renewable energy sector faces is to reduce the cost of energy. The cost of energy is strongly affected by the downtime of renewable energy power plants such as wind turbines or wave and tidal energy devices. Offshore renewable energy devices typically deal with large forces moving at a low speed making conventional high speed and low force generators unsuitable. These generators require a gearbox or other speed conversion mechanisms, which introduce additional risks of failure and maintenance requirements [1]. A major generator failure in offshore wind turbines can lead to several weeks of downtime [2]. Direct-drive generators eliminate the need for a gearbox, however they are very large and heavy, which increases their cost and complicates their transportation. Hence, for offshore applications, a compact, robust and modular generator, which can continue operating even under certain fault conditions, is desirable.

Axial flux generators in particular offer the possibility of stacking modules axially, several examples of multistage axial flux machines have been discussed in literature [3, 4]. Stacking the modules results in a NS-type machine, the flux for this machine travels mainly axially. Through this option, the possibility arises to reduce the active mass of the machine and maintain a smaller diameter generator at the cost of an increased axial length. However, another stacking option is available. Modules can be stacked concentrically on top of each other, which allows to have a large diameter machine with modular components. The two stacking options are applied to our double claw pole generator design to find the best stacking method for axial flux machines to further increase their power density.

The main features of the double claw pole machine can be described as follows [5]. It is a superconducting axial flux machine. High temperature superconducting (HTS) tapes are used for the field winding, HTS tapes allow for a very high current density, which increases the magnetic loading of the generator and makes it very compact. HTS bulks can also be used to develop superconducting machines, but their size is very limited [6-9]. HTS tapes can be wound into fielding windings of flexible size for a wide range of required power levels. Unlike the majority of other superconducting generator designs with rotating superconducting windings, the field winding of our design is stationary [10-17]. This eliminates the need for cryocouplers and brushes thereby increasing the reliability of the machine. Rotating claw poles are oriented around the field winding creating the NS pole variation across the stator teeth. The machine is highly modular. It features two stators on each side, which can operate independently in case of a fault. The field winding can be wound into separate loops with separate cryostats, hence even if one of the field windings has a fault the generator can continue to work under partial load. Detailed discussions on the generator's basic electromagnetic characteristics, such as electromotive force (EMF) and torque, can be found in [5, 18]. Table 1 provides a general summary of the double claw pole generator design such as dimensions and electrical characteristics.

Table 1

Double claw pole design

Total mass	184.2 t
Outer diameter	6.37 m
Poles	88
Stator coils per stator	66
Power output	10 MW
Line voltage	3.3 kV
Rotational speed	10 rpm
Power density	54.28 W/kg
Efficiency	94.50 %

The schematic of the double claw pole machine is shown in Fig. 1. A cross section of the generator is shown with one pole pair depicted.

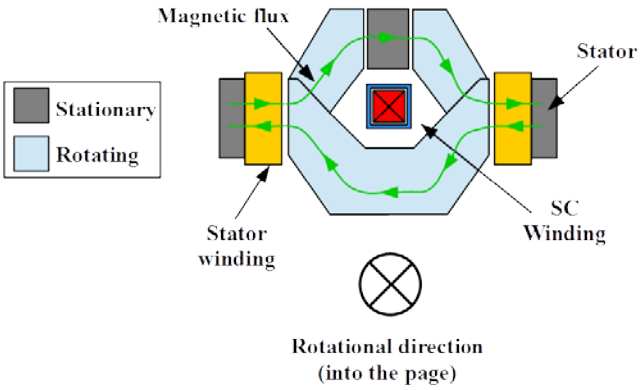

Fig. 1. *Concept of the double claw pole machine with superconducting field winding.*

2. Modelling of the stacking methods

2.1. Reluctance network model

In order to investigate the different stacking options, a reluctance network of the double claw pole machine was developed in MATLAB [19, 20]. The reluctance network is shown in Fig. 2. Each component of the machine is represented by several reluctances. Each reluctance is calculated according to its geometry and material properties using (1).

$$R = \frac{l_e}{\mu_0 \mu_r A} \quad (1)$$

where l_e is the equivalent length through the component, μ_0 is the permeability of air, μ_r is the relative permeability of iron and A is the cross-sectional area of the component.

It was decided to use Vacoflux50 for the active mass due to its high saturation limit of 2.28 T at 16 kA/m, the material datasheet was supplied by Vacuumschmelze [21]. It is a cobalt iron alloy, which is relatively expensive in comparison to other electrical steels. However, it allows high air gap flux densities without using an excess amount of superconducting tape. In addition, Vacoflux50 can be manufactured in laminations. Hence, even large machine components can be assembled.

In addition, all major leakage paths were considered such as, leakage flux between the claw poles and zig-zag leakage flux between stator teeth. Equation 2 shows the resulting reluctance matrix. A Newton-Raphson algorithm is used to solve the non-linear flux equations (Fig. 3).

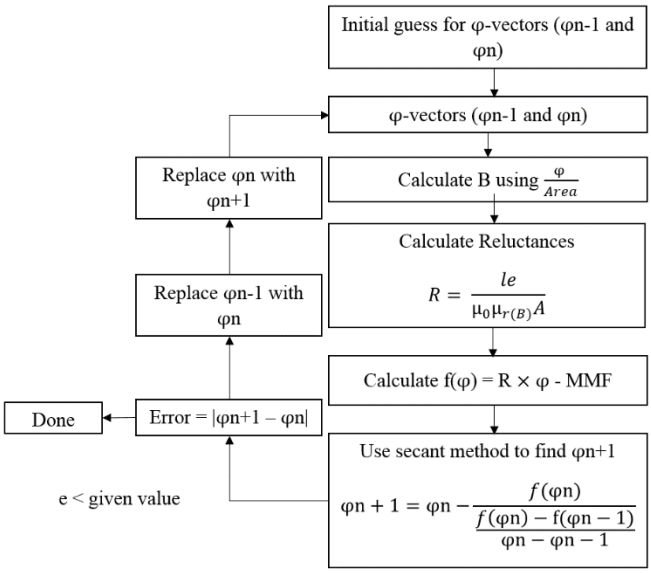

Fig. 3. *Algorithm used to solve the non-linear flux equations machine*

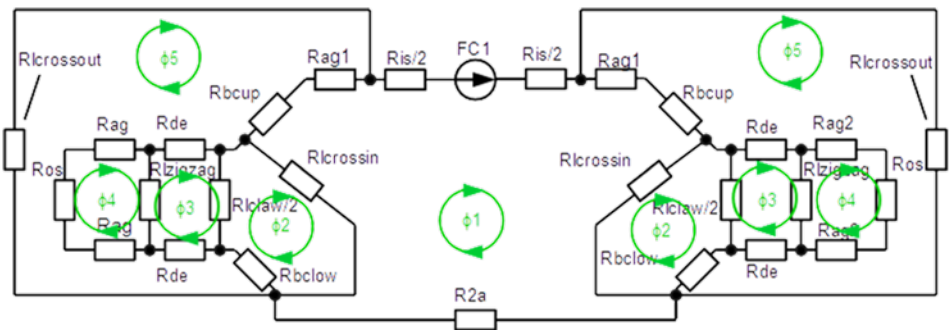

Fig. 2. *Reluctance network of the double claw pole machine*

$$\begin{bmatrix} 2\times(R_{iag}+R_{bup}+R_{lcrossin})+R_{2a}+R_{is} & -2\times R_{lcrossin} & 0 & 0 & -2\times(R_{iag}+R_{bup}) \\ -2\times R_{lcrossin} & 2\times(0.5\times R_{lclaw}+R_{blow}+R_{lcrossin}) & -R_{lclaw} & 0 & -2\times R_{blow} \\ 0 & -R_{lclaw} & 2\times(0.5\times R_{lclaw}+2\times R_{de}+R_{zigzag}) & -2\times R_{zigzag} & -4\times R_{de} \\ 0 & 0 & -2\times R_{zigzag} & 2\times(R_{zigzag}+2\times R_{oag}+R_{os1}+R_{os2}) & -2\times(2\times R_{oag}+R_{os1}+R_{os2}) \\ -2\times(R_{iag}+R_{bup}) & -2\times R_{blow} & -4\times R_{de} & -2\times(2\times R_{oag}+R_{os1}+R_{os2}) & 2\times(R_{lcrossout}+R_{blow}+2\times R_{de}+2\times R_{oag}+R_{iag}+R_{os1}+R_{os2}+R_{bup}) \end{bmatrix} \begin{bmatrix} \phi_1 \\ \phi_2 \\ \phi_3 \\ \phi_4 \\ \phi_5 \end{bmatrix} = \begin{bmatrix} MMF \\ 0 \\ 0 \\ 0 \\ 0 \end{bmatrix} \quad (2)$$

From the reluctance network, the stator tooth flux is obtained and hence the power output can be calculated. In addition to the reluctance network modelling, magnetostatic as well as transient analysis using the finite element analysis (FEA) software *Infolytica MagNet* was performed.

For both MATLAB and *Infolytica MagNet*, the $\mu_{r\,(B)}$ curve of Vacoflux50 [21] is used to calculate flux densities in the generator. The results are then compared for validation. The 3D finite element analysis (FEA) is used to verify the results from the reluctance network model. Using the stator tooth flux the power output of the stators is determined using (3).

$$P_{\mathrm{OUT}} = N_{\mathrm{COIL}} \times (E_{\mathrm{RMS}} \times I_{\mathrm{RMS}} - {I_{\mathrm{RMS}}}^2 \times R_{\mathrm{COIL}}) \quad (3)$$

where N_{COIL} is number of coils per stator, E_{RMS} is the induced voltage for one coil, I_{RMS} is the stator current and R_{COIL} is the resistance of a stator coil.
E_{RMS} can be calculated according to Faraday's law using (4).

$$E_{\mathrm{RMS}} = \frac{N_{\mathrm{TURN}} \times \phi_{\mathrm{PEAK}} \times f}{\sqrt{2}} \quad (4)$$

where N_{TURN} is the number of turns per coil, ϕ_{PEAK} is the peak stator tooth flux and f is the electrical frequency.
I_{RMS} is calculated using (5).

$$I_{\mathrm{RMS}} = J_{\mathrm{RMS}} \times A_{\mathrm{COIL}} \quad (5)$$

where J_{RMS} is the current density of copper which is assumed to be 5×10^6 A/m^2 and A_{COIL} is the area of a stator coil.

In conjunction with the developed reluctance network model the different stacking options can be investigated.

2.2. Axial stacking

Since the double claw pole machine is an axial flux machine, the possibility of stacking modules axially is available. Through this option, the possibility arises to reduce the active mass of the machine by partially eliminating the stator back iron that is shared between connecting modules. This is highlighted in Fig. 4. The figure shows a cross-section of the generator design, looking at one pole pair.

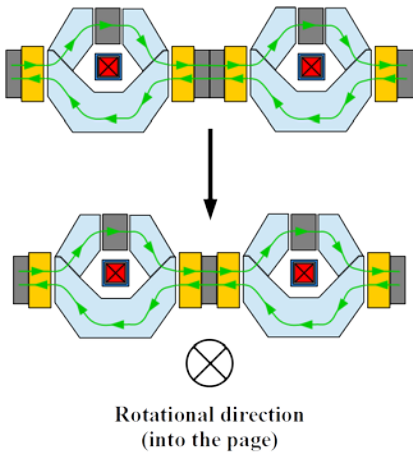

Fig. 4. *Axial stacking of the double claw pole machines, and structural optimization.*

As shown, two modules share the same stator back iron in the middle. Hence the active mass is reduced. Fig. 5 shows the full machine for this stacking method. Fig. 6 shows the reluctance network for 2 modules that was used for the axial stacking method. It is a combination of the original reluctance network (Fig. 2) with a shared stator in between the two modules.

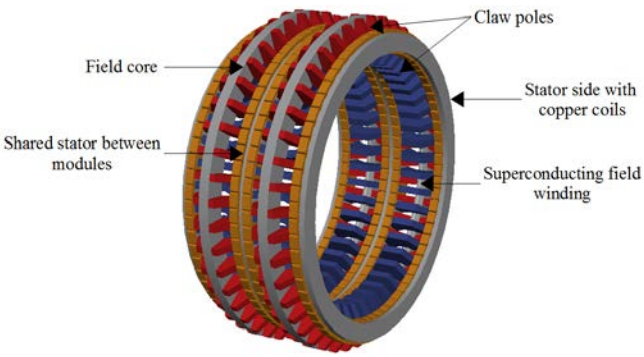

Fig. 5. *Full machine for stacking two modules axially*

2.3. Concentric stacking

Due to the structure of the double claw pole machine another stacking option is available. Modules can be attached concentrically on top of each other, as shown in Fig. 7.

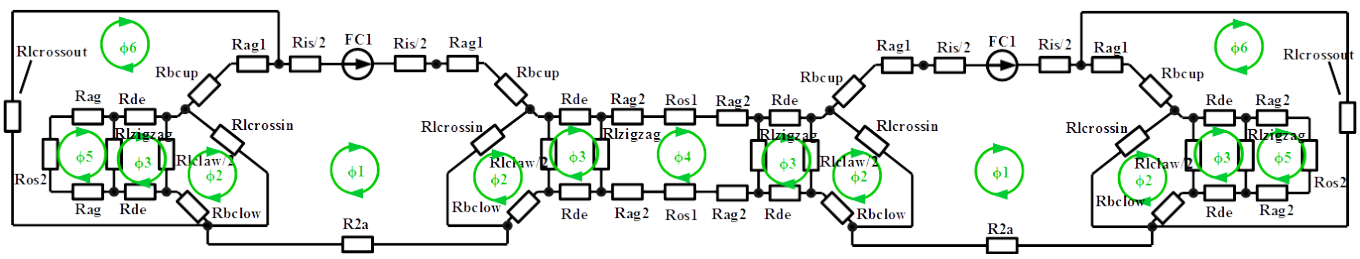

Fig. 6. *Reluctance network for axial stacking*

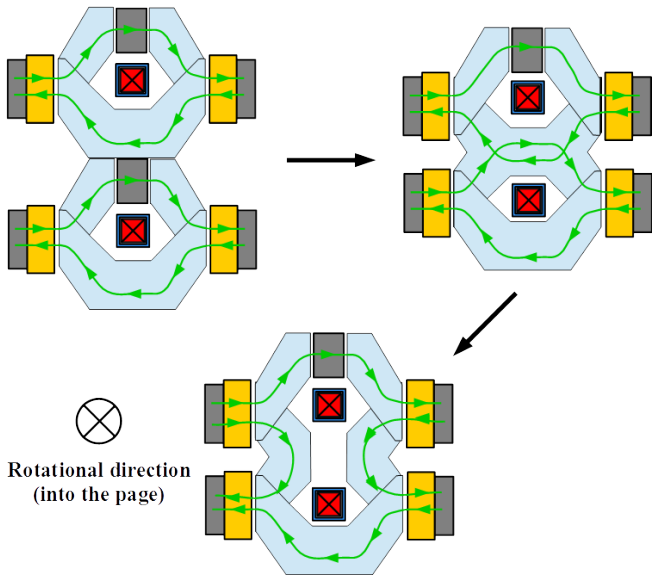

Fig. 7. *Concentric stacking of the double claw pole machines, and structural optimization.*

As can be seen, the middle section of the larger claw poles was eliminated since the magnetic fields produced by the field windings cancel each other in between them. A mass reduction of the claw poles is achieved. In addition, the air gap diameter of the machine increases with each additional module hence the power density is expected to increase significantly for this stacking method. The basic machine equation shown in (6) highlights that the power output is proportional to the air gap diameter squared.

$$P = BA_{\mathrm{E}}\frac{\pi}{2}D^2L\omega \quad (6)$$

where P is the output power, B is the magnetic loading, A_{E} is the electric loading, D is the air gap diameter, L is the axial length and ω is the rotational speed. For concentric stacking several air gap diameters exist, where the innermost air gap diameter would be D_1 and the outermost air gap diameter would be D_2 for a two-module machine design.

Another advantage that the concentric stacking option offers over the axial method is that it reduces the number of air gaps. For the original concept shown in Fig. 1 the magnetic flux crosses 6 air gaps before the loop is closed. Stacking the modules axially essentially doubles the original machine hence two axially stacked modules have 12 air gaps. Stacking the modules concentrically however eliminates one of the field cores. For 2 modules, the number of air gaps is reduced down to 10. Hence, the machine can be designed for a lower magnetomotive force (MMF), which reduces the amount of HTS tape that is required.

The flux path for this configuration can be described as follows. The magnetic flux travels from the first stator (bottom left) upwards over the middle claw pole into the upper stator. It then travels radially through the stator back iron. The flux then flows axially over the upper small claw poles and the field core to the right-hand side stator. It is then again guided downwards over the middle claw pole. The magnetic flux loop is closed over the bottom large claw pole. Fig. 8 shows the full machine for this stacking option.

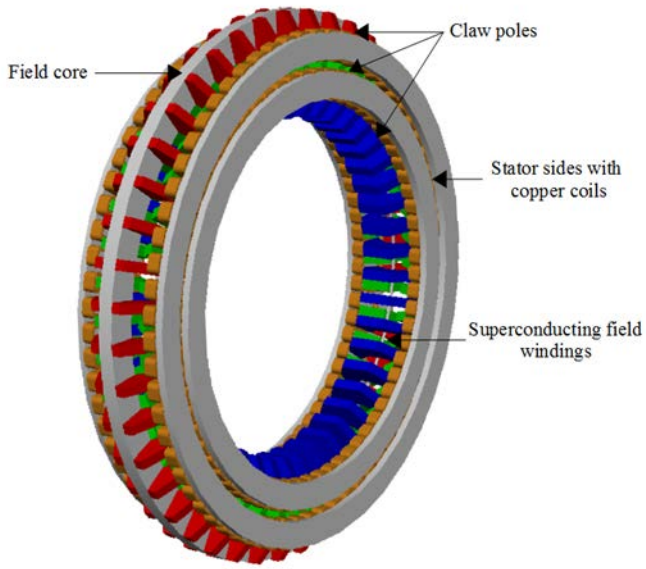

Fig. 8. *Full machine for stacking two modules concentrically*

Fig. 9 shows the reluctance network for 2 modules for the concentric stacking method. The original reluctance network was adjusted to represent the middle claw poles, which connect the lower and upper stators.

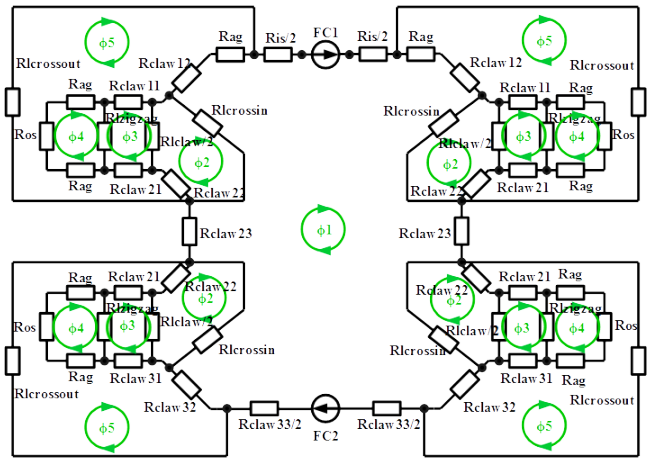

Fig. 9. *Reluctance network used for concentric stacking*

3. Results

3.1. Design of the 5 MW module

In order to compare the two methods, a 5 MW module was designed. The reluctance network shown in Fig. 2 was used for this task. The machine components were scaled down and adjusted until the desired power output of 5 MW was reached. The dimensions of the claw poles were chosen such as that iron saturation is avoided at rated MMF while minimizing active mass. Fig. 10 shows the stator tooth flux variation with MMF, as can be seen the machine starts saturating at approximately 23 kA×turns. The optimal MMF for a power output of 5 MW was found to be 22.4 kA×turns. With a transport current of 100 A, the resulting field winding results in 3 separately wound superconducting coils, connected in series and placed next to each other. Each coil

consists of 75 turns, giving a total number of turns of 225 for the superconducting field winding.

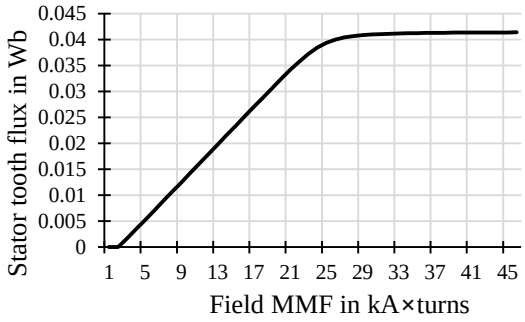

Fig. 10. *Stator tooth flux variation with MMF for the 5 MW module concentrically*

Table 2 shows a comparison between the 5 MW module and the full 10 MW double claw pole generator described in reference [5]. 88 poles in combination with 66 stator slots was found to give the highest efficiency. In addition, this combination of poles and stator slots creates rotational symmetry, which allows to only model a fraction of the generator and speeds up the computational time. In order to make a meaningful comparison, the rotational speed as well as the number of poles were kept the same for both generator designs.

Table 2

Comparison between 5MW module and full 10MW design

Power	5 MW	10 MW
Efficiency	93.76%	94.50%
RPM	10 rpm	10 rpm
Number of poles	88	88
Coils per stator	66	66
Active mass	36 t	58 t
Inner radius	1.91 m	2.29 m
Outer radius	2.66 m	3.19 m
Axial length	1.15 m	1.38 m
MMF	22400 A×turns	32400 A×turns
HTS tape length at 65K	7.56 km	13.5 km

In [22] the main design requirements of a 5 MW superconducting generator are discussed. To be economically as well as technically viable the target weight of the active mass of the generator was suggested to be below 40 tons to be competitive against permanent magnet technology. The maximum allowed HTS tape was calculated to be 228 km of AMSC 348C that has a critical current of 95 A at 77 K, or 206 km of Superpower tape 4050 with a critical current of 125 A at 77 K, to be economically feasible. As can be seen the 5 MW module satisfies both requirements. At 65 K the generator design requires 7.56 km of superconducting tape at an operating current of 100 A. This can be further reduced by lowering the operating temperature to 20 K which reduces the tape requirements to 1.89 km with an operating current of 400 A.

The required cooling power for both temperatures can be estimated to be approximately 125 W [5]. Since it is more challenging to remove heat at a lower temperature, the required input power to the cooling system is significantly larger for 20 K as compared to 65 K [23]. In addition, operating at low temperatures such as 20 K or even 10 K requires a large number of cooling heads making these designs impractical [6]. To maintain a higher efficiency and a simplified cooling system, 65 K was chosen as the operating temperature, at the cost of increased superconducting tape requirements. Superconductors generate loss within the machine environment even conducting DC currents [24-26]. This requires further discussion and will be presented in our other papers.

In order to validate the 5 MW design of the double claw pole machine module a 3D finite element analysis was performed using the simulation software *Infolytica MagNet*. The total flux density distribution in the machine is shown in Fig. 11. The air gap flux density distribution is shown in Fig. 12. The figure shows the distribution for cases, when the large claw pole (lower claw pole) and when the small claw pole (upper claw pole) are aligned with the middle stator tooth.

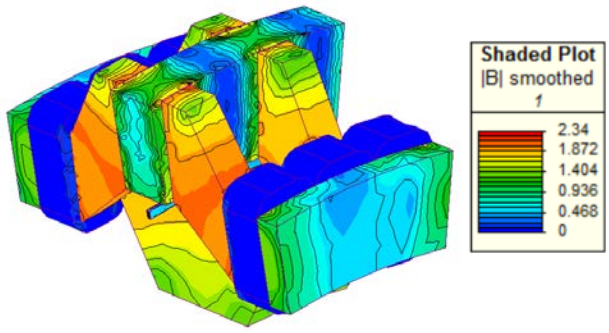

Fig. 11. *Total flux density distribution for the 5 MW module*

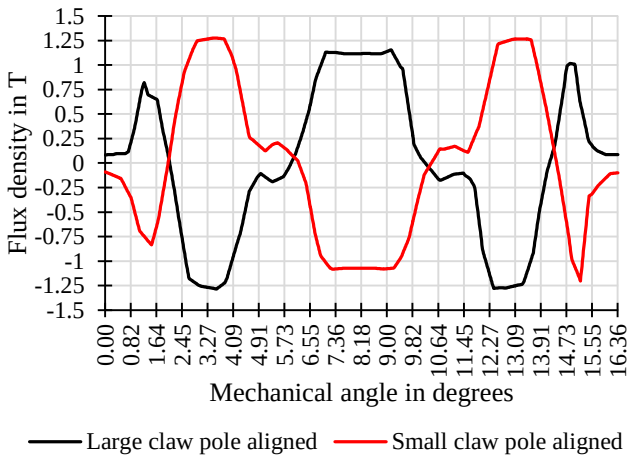

Fig. 12. *Air gap flux density distribution for large and small claw poles aligned with middle stator tooth*

The stator tooth flux was calculated to be equal to 0.038 Wb, which is in good agreement with the reluctance network model, which found the flux to be equal to 0.037 Wb. Fig. 13 highlights the open-circuit voltage of the 5 MW generator design for 6 stator coils. An in-phase voltage is induced in the coils that are oriented opposite of each other, hence there are always 2 curves overlapping

each other. The period of the voltage is 136.36 ms, which gives an electrical frequency of 7.33 Hz at 10 rpm. There are 66 coils in total per stator, each coil has 96 turns. Each phase consists of two parallel branches of 11 coils in series.

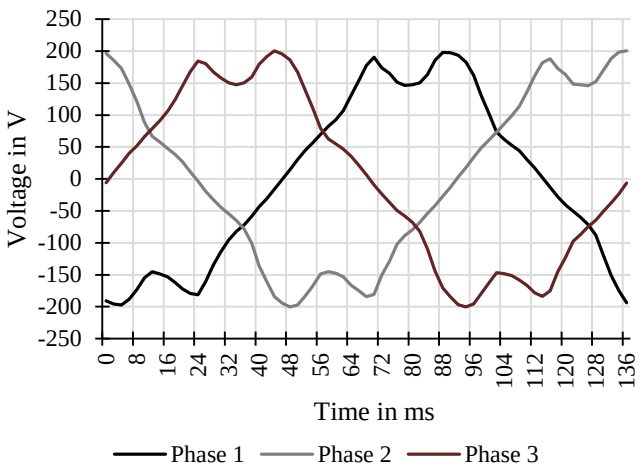

Fig. 13. *Open-circuit voltage for the 5 MW module*

3.2. Comparison between stacking methods

The two stacking methods are then applied in conjunction with the 5 MW modules. Fig. 14 shows the performance comparison between the two methods.

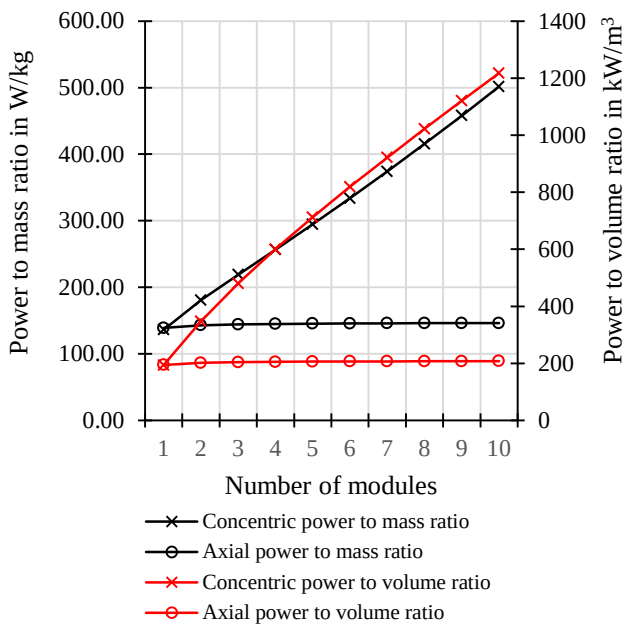

Fig. 14. *Power density comparison between concentric and axial stacking*

For the axial stacking method, the power density in terms of mass and volume does not change significantly since only a small portion of the active mass is eliminated. Stacking the modules concentrically however increases the power density considerably in both aspects since the air gap diameter increases with every new module. Especially in terms of power to volume ratio, a very high power density machine can be assembled by stacking modules on top of each other. For instance, stacking two modules concentrically creates a 12.1 MW machine with an outer diameter of 6.2 m, which is smaller than the 10 MW machine, which has an outer diameter of 6.38 m. This makes the concentric modules an attractive option for high power density applications and applications where space is an issue.

Another important aspect for generators is their efficiency. The main losses such as the cooling power for the superconductor cryostat, iron losses and copper losses were considered. Due to the low frequency the iron losses are relatively low and the overall efficiency is dominated by the copper losses in the stators. For the superconducting field winding the following losses were considered, suspension straps fixing the winding within the cryostat, radiation, current leads, cold-head sleeve and eddy currents. Initial results show that the losses of the superconducting tapes are expected to be very low, since these tapes only carry DC currents. However, detailed modelling of the field winding is necessary and will be carried out to quantify the losses and to identify potential hot spots. Fig. 15 shows the efficiency variation for the two stacking options.

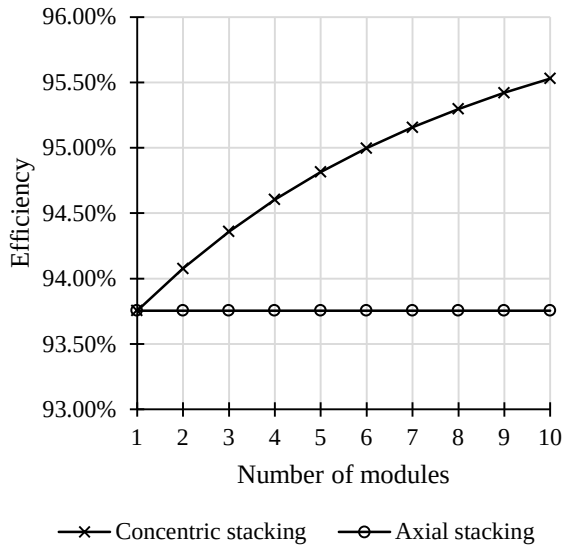

Fig. 15. *Efficiency for stacking modules axially and concentrically*

For the axial stacking method, the efficiency is constant since each module produces power at the set efficiency of 93.76%. When stacking the modules concentrically the efficiency changes since the power output for each additional module varies. The efficiency is calculated separately for each module and by using the contribution towards the total power output from each module the overall efficiency of the whole generator is calculated.

Table 3 shows a comparison between the two stacking methods for two modules and the original 10 MW design of the double claw pole machine. Each design has 88 poles and runs at 10 rpm. When stacking the modules concentrically the generator offers better performance. The power density in terms of mass as well as volume was improved in comparison to the original 10 MW design while maintaining approximately the same HTS tape requirements. One disadvantage of the stacking methods is that the efficiency is lower than for the original generator.

Table 3

Comparison between stacking methods and original 10 MW design

Design	Concentric stack	Axial stack	Original
Power	12.1 MW	10 MW	10 MW
Power density (mass)	183.3 W/kg	142.9 W/kg	172.4 W/kg
Power density (volume)	348.5 kW/m^3	203.5 kW/m^3	226.7 kW/m^3
Efficiency	94.08%	93.76%	94.5%
Active mass per 10 MW	54.5 t	70 t	58 t
Inner radius	1.91 m	1.91 m	2.29 m
Outer radius	3.10 m	2.66 m	3.19 m
Axial length	1.15 m	2.21 m	1.38 m
MMF	36,600 A×turns	44,800 A×turns	32,400 A×turns
HTS tape length at 65K	13 km	15.12 km	13.5 km

3.3. Validation using finite element analysis

To confirm the results from the reluctance models, a 3D finite element analysis (FEA) for each stacking method was performed using the simulation software *Infolytica MagNet*. Since the flux travels three-dimensionally it is essential to use 3D FEA in order to simulate the machine accurately. One quarter symmetry was applied in order to reduce the computational time. The mesh size was reduced in the air gaps of the generator in order to improve the accuracy of the results. Fig. 16 and 17 show the flux density distributions for the stacking options. Fig. 16 highlights the total flux density in the machine for axial stacking. Evidently, the claw poles start saturating around the elbow, this indicates that the MMF was chosen adequately.

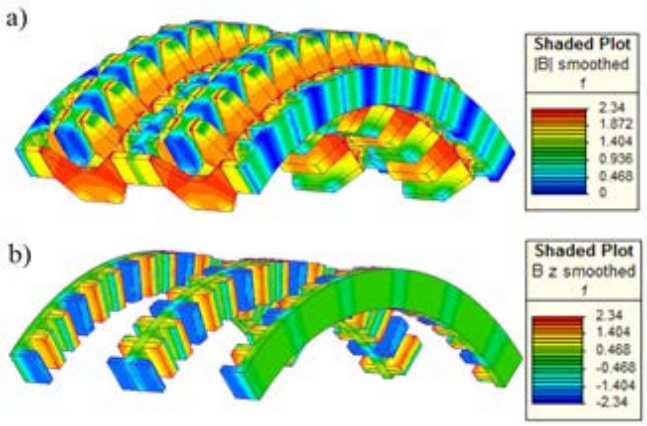

Fig. 16. *a) Total flux density distribution and b) z-direction flux density distribution in the stator teeth for axial stacking (i.e. out/into the stator teeth)*

The figure also shows the z-direction flux density, i.e. the flux in and out of the stator teeth, when the bottom larger claw pole is aligned. The z-direction flux density for the stator teeth was found to be equal to 1.38 T. The stator tooth flux density from the reluctance network model was calculated to be 1.32 T, showing a good correlation between the FEA and the reluctance model.

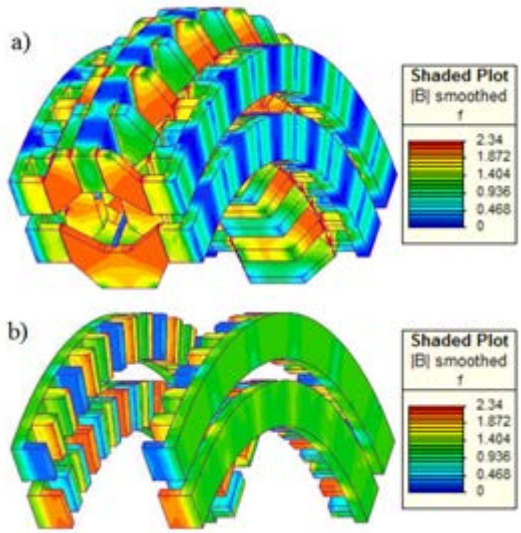

Fig. 17. *a) Total flux density distribution and b) z-direction flux density distribution in the stator teeth for concentric stacking (i.e. out/into the stator teeth)*

Fig. 17 shows the total flux density distribution when stacking modules concentrically, similarly to the axial stacking method, the elbows of the claw poles are saturated. The figure also shows the z-direction flux density. The stator tooth flux density for the lower and upper stators were found to be equal to 1.3 T when overlapping with the outer claw poles, similar to stacking the modules axially. From the reluctance model, the stator tooth flux for both stators was found to be equal to 1.32 T again showing a good correlation between the two models.

Additionally, it is important to analyse the machine performance under no load and load conditions. Figure 18 shows a cogging torque comparison for the original design and the two stacking methods over one period. For 10 MW and 10 RPM the rated torque for the generator is 9.55 MNm. The original design has the lowest cogging with a peak of -56 kNm, the concentric stacking method has a peak of -61 kNm and the axial stacking method results in the highest cogging torque with a peak of -94 kNm.

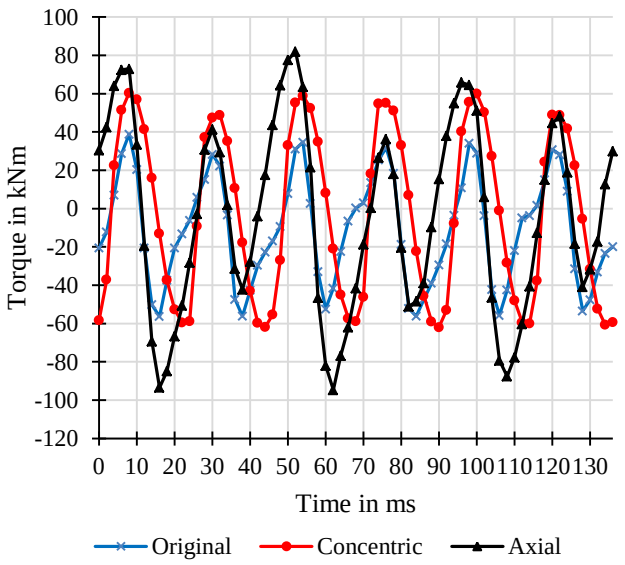

Fig. 18. *Cogging torque over one cycle for the original design and both stacking methods*

The cogging torque for the concentric stacking method is lower than for the axial stacking method since the concentric method results in only 10 air gaps instead of 12 as mentioned in section 2.3. While both stacking methods resulted in a higher cogging torque, it should be noted that the original design was optimized through a genetic algorithm optimization tool [5]. The cogging torque for both stacking methods could be further decreased through applying optimization tools.

Under load conditions the torque ripple was found to be 12.2 % for the original design, 14.3 % for the concentric design and 14.8 % for the axial stacking method. The cogging torque and torque ripple were found to be relatively high for the original design as well as each newly proposed design. This is mainly due to the combination of number of poles and stator slots. To achieve a low cogging torque and torque ripple a large least common multiple is desirable between the number of poles and stator slots [27]. However, a small least common multiple creates rotational symmetry and allows for modelling only a fraction of the full generator. The designs introduced in this paper have a small least common multiple with 88 poles and 66 slots to take advantage of rotational symmetry and reduce the computational time. The designs introduced can be optimized by choosing a more suitable combination of poles and stator slots to decrease the cogging torque and torque ripple. In addition, the torque characteristics can be further improved by skewing the stator teeth [28].

Figure 19 highlights the induced coil voltages for each proposed design when supplying a purely resistive load. For the original and the axial design, one power converter can be used since the phase voltages are of the same magnitude and phase. For the concentric method two power converters are required since the voltages produced by the bottom and top modules are of different magnitudes and phase.

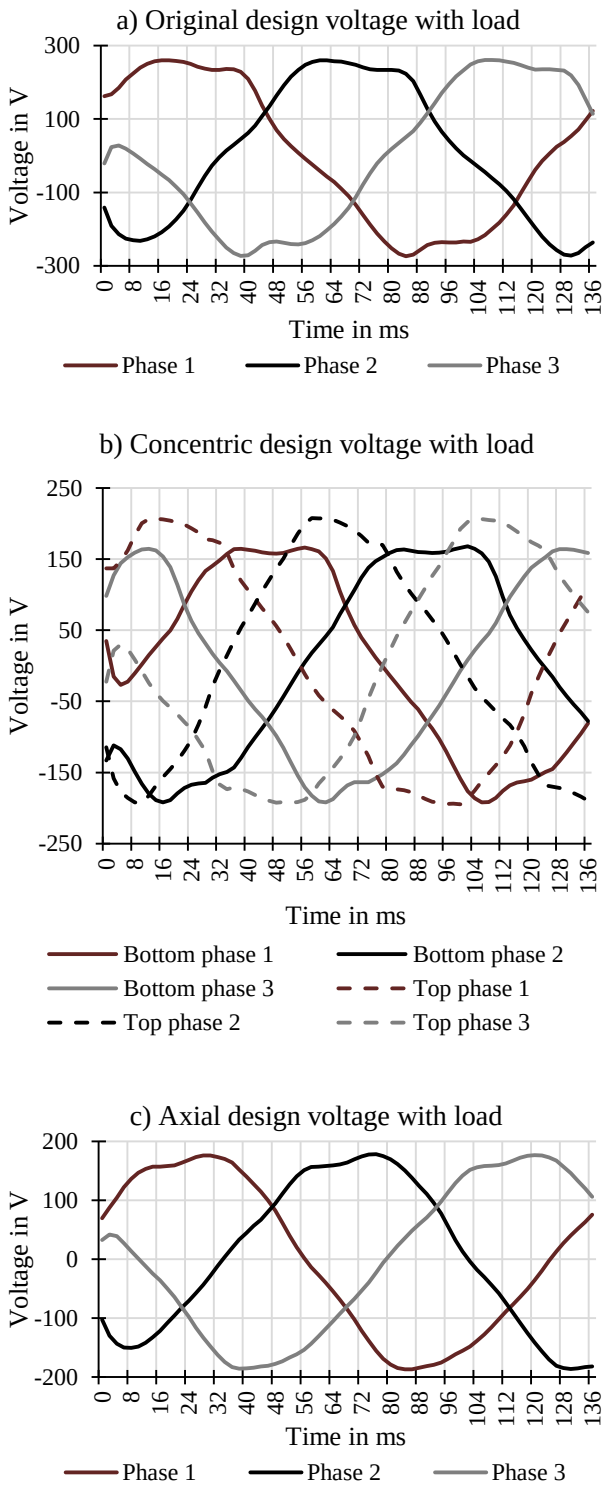

Fig. 19. *Induced voltage with a resistive load for a) the original design, b) the concentric design and c) the axial design*

It was shown that two stacking options can be applied to an axial flux machine. Both options further increase the modularity and power density of the machine without compromising the torque characteristics of the generator. From a manufacturing point of view, there are significant advantages to be gained by manufacturing standardized modules. The manufacturer only needs to produce a certain set of components that can then be

assembled to create a machine with the desired power output. The machine components are more compact and easier to handle than if one big machine was developed. The smaller machine components also reduce the construction costs of the generator when compared to conventional generators. In [29] the cost of a 6 MW permanent magnet generator for large wind turbines is discussed for different drive-train configurations such as, direct-drive, single-stage and multi-stage gearboxes. Table 4 summarizes the associated costs for each drive-train configuration [29].

Table 4
6 MW permanent magnet generator (PMG) cost comparison

	DD PMG	**PMG 1G**	**PMG 2G**	**PMG 3G**
Generator specifications				
Generator speed (rpm)	12	96	480	1200
Gearbox ratio	-	1:8	1:40	1:100
Stator radius (m)	3.5	2.5	0.7	0.5
Stack length (m)	1.5	0. 4	0.8	0.9
Cost (k€)				
Generator active material	330	77	39	38
Generator construction	436	115	24	10
Gearbox	-	672	1170	1330
Generator system cost	**766**	**864**	**1233**	**1378**

As can be seen, the generator construction cost significantly decreases with generator size. The direct-drive generator discussed in the paper has a stator radius of 3.5 m and the construction cost was estimated to be 436,000 €. The generator with a single-stage gearbox has a stator radius of 2.5 m and the construction cost for this case was estimated to be 115,000 €. It was shown that the generator construction cost significantly decreases with size. The concentric direct-drive 12 MW generator design proposed in this paper has an outer radius of 3.1 m, making it smaller than a conventional direct-drive generator of half the power rating. Due to the smaller machine dimensions the construction cost of the proposed design is expected to be significantly lower than that of a conventional generator and in combination with the small amount of HTS tape required, the proposed design is considered a very competitive option in terms of cost and performance. Further discussion on the construction of the double claw pole machine can be found in [28].

The smaller and lighter components also simplify the transportation of the machine, this is especially important for offshore renewable energy applications [30, 31]. Another advantage of the modular setup is that an existing axial flux machine can be upgraded to a higher power rating by adding another module without the need of investing in a completely new machine. Stacking several modules on top of each other however results in very large diameter machines. For 5 modules the outer diameter is 8.76 m with a power rating of 49.5 MW. Here the possibility arises to lay out the machine horizontally. This is especially interesting for hydro power plants.

4. Conclusion

Highly modular machines are desirable because they are easier to manufacture and transport. This is especially important for offshore renewable energy applications where transportation and assembly of very large generators can be an issue. In addition, modular machines offer redundancy and can keep operating even under certain fault conditions. While the double claw pole machine was already found to be highly modular, a further improvement was considered. A 5 MW standardized module of the double claw pole machine was designed and the option of stacking these modules axially and concentrically was explored. Both options were found to increase the power density in terms of mass as well as volume. Stacking the modules concentrically however was found to offer significant advantages. For concentric stacking, each additional module increases the air gap diameter of the machine hence increasing the power output significantly. In addition, the MMF requirements for this method are lower than for the axial stacking method since stacking the modules concentrically allows for eliminating two air gaps. It was shown that stacking two modules concentrically results in a more compact machine than the original 10 MW design of the double claw pole generator.

Acknowledgments

This work was supported by the Engineering and Physical Sciences Research Council [Grant number: EPSRC EPN509644/1].

References

[1] Keysan, O., Mueller, M., McDonald, A., et al.:"Designing the C-GEN lightweight direct drive generator for wave and tidal energy", *IET Renewable Power Generation*, vol. 6, no. 3, pp. 161 - 170, 2012.

[2] Faulstich, S., Hahn, B. and Tavner, P. J.: "Wind turbine downtime and its importance for offshore development", *Wind Energy*, vol. 14, no. 3, pp. 327-337, 2011.

[3] Keysan, O., McDonald, A., Mueller, M., et al.:"C-GEN, a lightweight direct drive generator for marine energy converters", in *5th IET International Conference on Power Electronics, Machines and Drives (PEMD 2010)*, Brighton, UK, 2010.

[4] Chan, A., Nilssen, R. and Nysveen, A.: "Performance Comparisons Among Radial-Flux, Multistage Axial-Flux, and Three-Phase Transverse-Flux PM Machines for Downhole Applications", *IEEE Transactions on Industry Applications*, vol. 46, no. 2, pp. 779 - 789, 2010.

[5] Keysan, O. and Mueller, M.: "A modular and cost-effective superconducting generator design for offshore wind turbines", *Superconductor Science and Technology*, vol. 28, no. 3, p. 034004, 2015.

[6] Nishimura, T., Nakamura T., Li, Q., et al.: "Potential for Torque Density Maximization of HTS Induction/Synchronous Motor by Use of Superconducting Reluctance Torque", *IEEE Transactions on Applied Superconductivity*, Vol. 24, No. 3, 5200504, 2014.

[7] Yan, Y., Hong, Z., Li, Q., et al.: "Thermally Actuated Magnetization Method in High Temperature Superconductor Bulks", *IEEE Transactions on Applied Superconductivity*, Vol. 20, No. 3, 2010.

[8] Li, Q., Yan, Y., Rawlings, C., et al.: "Numerical Analysis of Thermally Actuated Magnets for Magnetization of Superconductor", *Journal of Physics: Conference Series*, Vol. 234, 032035, 2010.

[9] Li, Q., Yan, Y., Rawlings, C., et al.: "Magnetization of Bulk Superconductors Using Thermally Actuated Magnetic Waves", *IEEE Transactions on Applied Superconductivity*, Vol. 20, No. 4, 2010.

[10] Hoang, T.-K., Quéval, L., Berriaud, C., et al.: "Design of a 20-MW Fully Superconducting Wind Turbine Generator to Minimize the Levelized Cost of Energy", *IEEE Transactions on Applied Superconductivity*, vol. 28, no. 4, 2018.

[11] Mariono, I., Pujana, A., Sarmiento. G., et al.: "Lightweight MgB2 superconducting 10 MW wind generator", *IOPScience: Superconductor Science and Technology*, vol. 29, no. 2, pp. 1-11, 2016.

[12] Nam, G.-D., Sung, H.-J., Go, B.-S., et al.: "Design and Comparative Analysis of MgB2 and YBCO Wire-Based-Superconducting Wind Power Generators", *IEEE Transactions on Applied Superconductivity*, vol. 28, no. 3, 2018.

[13] Abrahamsen, A. B., Mijatovic, N., Seiler, E., et al.: "Superconducting wind turbine generators", *IOPscience: Superconductor Science and Technology*, vol. 23, no. 3, pp. 1-8, 2010.

[14] Snitchler, G., Gamble, B., King, C., et al.: "10 MW Class Superconductor Wind Turbine Generator", *IEEE Transactions on Applied Superconductivity*, vol. 21, no. 3, pp. 1089-1092, 2011.

[15] Fair, R., Stautner, W., Douglass, M., et al.: "Next generation drive train-superconductivity for large-scale wind turbines", in *Applied Superconductivty Conf.*, Portland, Oregon, 2012.

[16] Sung, H.-J., Kim, G.-H., Kim, K., et al.: "Practical Design of a 10 MW Superconducting Wind Power Generator Considering Weight Issue", *IEEE Transactions on Applied Superconductivity*, vol. 23, no. 3, 2013.

[17] Terao, Y. and Sekino, M.: "Electromagnetic Design of 10 MW Class Fully Superconducting Wind Turbine Generators", *IEEE Transactions on Applied Superconductivity*, vol. 22, no. 3, p. 5201904, 2012.

[18] Kails, K., Li, Q., Mueller, M.: "Novel model of stator design to reduce the mass of superconducting generators", *Superconductor Science and Technology*, vol. 31, no. 5, 2018.

[19] Kails, K., Li, Q., Mueller, M., "Mass reduction of superconducting power generators for large wind turbines", *The Journal of Engineering*, vol. 2019, no. 17, 2019.

[20] Bernholz, J. J. and Mueller, M.: "Analytical model of Superconducting Generators for Wave Energy Systems", in *8th IET International Conference on Power electronics, Machines and Drives*, Glasgow, 2016.

[21] Vacuumschmelze, "Vacoflux datasheet", 2017. [Online]. Available at http:\\www.vacuumschmelze.com

[22] Abrahamsen, A.B., Jensen, B., Seiler, E., et al.: "Feasibility study of 5 MW superconducting wind turbine generator", *Physica C*, vol. 471, no. 21-22, pp. 1464-1469, 2011.

[23] Kasap, S. and Capper, P.: "Springer Handbook of Electronic and Photonic Materials", Springer, 2017, p. 1227.

[24] Li, Q., Yao, M., Jiang, Z., et al.: "Numerical modelling of dyanmic loss in HTS-coated conductors under perpendicualr magnetic fields", *IEEE Transactions on Applied Superconductivity*, vol. 28, no. 2, pp. 1-6, 2018.

[25] Jiang, Z., Zhou, W., Li, Q., et al.: "The dynamic resistance of YBCO coated conductor wire: effect of DC current magnitude and applied field orientation", *Superconductor Science and Technology*, vol. 31, no. 3, 035002, 2018.

[26] Jiang, Z., Zhou, W., Bumby, C.W., et al, "Dynamic resistance measurement of a four-tape YBCO stack in a perpendicular magnetic field", *IEEE Transactions on Applied Superconductivity*, vol. 28, no. 4, pp. 1-5, 2018.

[27] Jiang, S., Zhu, Z. and Chan, C.: "Analytical methods for minimizing cogging torque in permanent-magnet machines", *IEEE Transactions on Magnetics*, vol. 45, no. 4, pp. 2023-2031, 2009

[28] Burchell, J.: "Advancement of direct drive generator systems for offshore renewable energy production, " The University of Edinburgh, PhD thesis available at: https://www.era.lib.ed.ac.uk/handle/1842/33263, 2017

[29] Hart, K., McDonald, A., Polinder, H., et al.: "Improved cost of energy comparison of permanent magnet generators for large offshore wind turbines", European Wind Energy Association Conference and Exhibition, 2014.

[30] Hassan, G. G.: "A Guide to UK Offshore Wind Operations and Maintenance", Scottish Enterprise and The Crown Estate, 2013.

[31] Cotrell, J., Stehly, T., Johnson, J., et al.: "Analysis of Transportation and Logistics Challenges Affecting the Deployment of Larger Wind Turbines: Summary of Results", NREL, 2014.